The rapid and cost-effective capture and subsurface mineral storage of carbon and sulfur at the CarbFix2 site

Ingvi Gunnarsson[1*], Edda S. Aradóttir[1], Eric H. Oelkers[2,3,4], Deirdre E. Clark[4], Magnús Þór Arnarsson[5], Bergur Sigfússon[1], Sandra Ó. Snæbjörnsdóttir[4,1], Juerg M. Matter[6,7], Martin Stute[7], Bjarni M. Júlíusson[8], and Sigurður R. Gíslason[4]

[1]Reykjavik Energy, Reykjavik, Iceland.

[2]GET, CNRS/UMR5563, Toulouse France.

[3]Earth Sciences, University College London, United Kingdom.

[4]Institute of Earth Sciences, University of Iceland, Reykjavik, Iceland.

[5]Mannvit Engineering, Reykjavík, Iceland.

[6]Ocean and Earth Science, University of Southampton, Southampton UK.

[7]Lamont-Doherty Earth Observatory, Columbia University, Palisades, USA.

[8]ON Power, Reykjavík, Iceland.

*Correspondence to: ingvi.gunnarsson@or.is

Abstract - One of the main challenges of worldwide carbon capture and storage (CCS) efforts is its cost. As much as 90% of this cost stems from the capture of pure or nearly pure CO_2 from exhaust streams. This cost can be lowered by capturing gas mixtures rather than pure CO_2. Here we present a novel integrated carbon capture and storage technology, installed at the CarbFix2 storage site at Hellisheiði, Iceland that lowers considerably the cost and energy required at this site. The CarbFix2 site, located in deeper and hotter rocks than the original CarbFix site, permits the continuous injection of larger quantities of CO_2 and H_2S than the original site. The integrated process consists of soluble gas mixture capture in water followed by the direct injection of the resulting CO_2-H_2S-charged water into basaltic rock, where much of the dissolved carbon and sulfur are mineralized within

months. This integrated method provides the safe, long-term storage of carbon dioxide and other acid gases at a cost of US $25/ton of the gas mixture at the CarbFix2 site and might provide the technology for lower CCS cost at other sites.

1. Introduction

The "Achilles heel" of carbon capture and storage (CCS) is its cost. Cost estimates range from US $38 to US $143/ton CO_2 (Global CCS Institute, 2011; Rubin et al., 2015). Here we describe an integrated method that substantially lowers this cost at the CarbFix2 storage site. This technology is based on the success of the rapid and safe subsurface mineralization of carbon and sulfur into basaltic rocks as a dissolved aqueous phase at the original CarbFix site (Matter et al., 2016; Snæbjörnsdóttir et al., 2017). Moreover, the cost of this CCS method in the present study is offset by the cost of sulfur fixation, which can exceed US $300/ton (U.S. Department of Energy, 2013). As such, this integrated method may provide the financial incentive for the general application of capturing and injecting gas mixtures into reactive rocks at other locations.

The present study builds on the original CarbFix project (Matter et al., 2016). The CarbFix approach is to accelerate the mineralization of injected acid gases into subsurface basaltic reservoirs. Carbon mineralization is the safest way of storing carbon in the subsurface (Benson et al. 2005; Gislason and Oelkers, 2014; Snæbjörnsdóttir et al., 2017). Basalt offers numerous advantages for the mineralization of CO_2 and other acid gases, as it is relatively reactive compared to most rocks, and its dissolution both liberates divalent metal cations such as Ca, Mg, and Fe, and helps neutralize acidic waters (Wolff-Boenisch et al., 2004; 2006; McGrail et al., 2006; Oelkers et al., 2008; Gislason et al., 2010; Gysi and Stefansson, 2012; Pham et al., 2012; Rosenbauer et al., 2012; Takazo et al., 2013; Schaef et al., 2013; 2014; Maskell et al., 2015; Gysi, 2017; Kanakiya et al., 2017; Luhmann, et al., 2017; Xiong et al., 2017; Snæbjörnsdóttir et al., 2018). The original CarbFix project injected 175 tons of pure CO_2 into subsurface porous basalts from January to March 2012, then 73 tons of a gas mixture from the Hellisheiði power plant consisting of 75 mol% CO_2, 24 mol% H_2S and 1 mol% H_2 from June to August 2012 (Alfredsson et al., 2013; Matter et al., 2016; Snæbjörnsdóttir

et al., 2017). In each case, the gases were dissolved into formation water during their injection (Gislason et al., 2010; Kervevan et al., 2014, 2017; Tao and Bryant, 2014; Sigfusson et al., 2015; Blount, et al., 2017). A combination of chemical and tracer analyses, geochemical calculations, and physical evidence demonstrated that the injected CO_2 and H_2S were fixed in minerals, notably calcite and iron sulfide minerals within two years of injection at 20-50°C (Matter et al., 2016; Snæbjörnsdóttir et al., 2017). The present study was motivated to upscale this process toward the economically viable capture and storage of all the acid gases emitted from the Hellisheiði geothermal power plant. The purpose of the present communication is to report the results of our efforts to upscale the mineralization of CO_2 and H_2S in basaltic rocks at Hellisheiði and to explore the possibility of adopting a similar approach at other potential CCS sites.

2. Materials and Methods

2.1 Capture and injection into the subsurface of the CO_2/H_2S charged fluid

Efforts in this study were based at the CarbFix2 injection site located approximately 1.5 km north of the Hellisheiði geothermal power plant (Fig. 1). The Hellisheiði geothermal field is equipped with over 100 vertical and diverted wells to varying depths ranging from 100 to 3300 m in depth, allowing for the detailed monitoring of the fate of fluids injected into the subsurface (Gunnlaugsson et al., 2012). The HN-16 CarbFix2 injection well, as well as the HE-31, HE-48, and HE-44 monitoring wells used in this study are directionally drilled to depths of 2204 m, 2703 m, 2248 m, and 2606 m, respectively, such that they intersect high permeability fractures at depths below 800 m.

The Hellisheiði field is located at the southern part of the Hengill volcanic system, which was formed by several volcanic cycles during spreading episodes in the rift zone. The Hengill central volcano occupies the central part of a 60-100 km long and 3-5 km wide volcanic NE-SW trending fissure swarm with a graben structure. The CarbFix2 site is located at the western side of the graben structure, with large normal faults having a total throw of more than 300 m (Franzson et al., 2010; Franzson et al., 2005, Fig. 1). These faults contribute significantly to the permeability in the area (Kristjánsson, et al., 2016).

The subsurface rocks at the CarbFix2 injection site consist of olivine tholeiitic basalts. The top 1000 m are dominated by hyaloclastites erupted sub-glacially. The hyaloclastites are heterogeneous and can range from crystalline rocks with minor amounts of volcanic glass to almost solely volcanic glass. In the less mountainous parts of the system the stratigraphy consists of alternating successions of hyaloclastite formations and lava sequences. The most prominent originate from large lava shields which erupted in the highlands and flowed to the surrounding lowlands (e.g. Franzson et al., 2010). Olivine tholeiitic lavas are usually rich in volcanic glass, especially on rapidly chilled surfaces of lava flows. Intrusive rocks dissect these hyaloclastite/lava successions below about 800 m depth and become dominant below 1700 m. These intrusive rocks contribute substantially to the subsurface permeability and the fracture networks created by their emplacement is a major control on aquifer permeability below 500 m (e.g. Franzson, 1988). The temperature at the ~2000 m depth of the target acid gas storage reservoir ranges from 220 to 260 ^{o}C. At this depth chlorite, epidote, and calcite are the most common secondary minerals, together with prehnite, sulphides, wollastonite, and actinolite (Snæbjörnsdóttir, 2011).

Note the temperature of the target aquifer of the CarbFix2 injection is substantially higher than that of the original CarbFix injection. This higher temperature offers advantages and disadvantages compared to the lower temperature injection. First, the higher temperature of the CarbFix2 target aquifer limits the risk of subsurface biotic activity that might influence the injection well and aquifer injectivity (Trias et al., 2017). Second, the rates of basalt dissolution and of mineral carbonation reactions increase with increasing temperature (Gislason and Oelkers, 2003; Gudbrandsson et al., 2011). This effect will be offset somewhat by the decreasing thermodynamic drive for carbonate mineral formation with increasing temperature. For example, calcite and quartz decompose into wollasonite, liberating CO_2 at temperatures exceeding 325 ^{o}C (Skippen, 1980; Snæbjörnsdóttir et al., 2014). Due to these competing effects, some have suggested that the optimal temperature for subsurface mineral carbonation occurs at approximately 185 ^{o}C (e.g. Gerderman et al., 2002; Keleman and Matter, 2008).

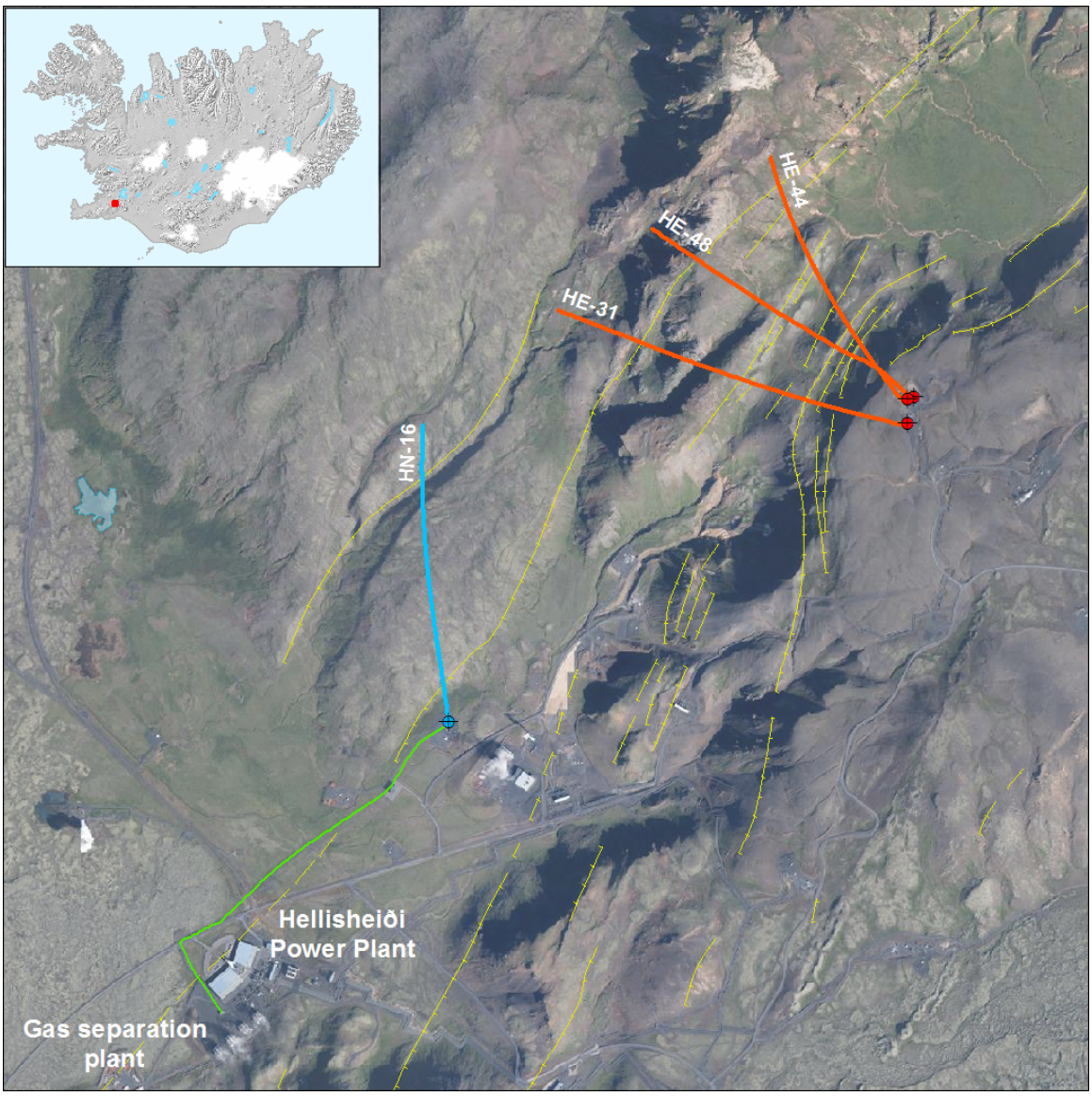

Fig 1. Overview of the CarbFix2 injection site. The Hellisheiði power plant and the gas separation plant are in the lower left of the figure. The 1.5 km long, gas charged water pipe (shown in green) connects the separation plant to the injection well. Injection was into well HN-16 (shown in blue), three monitoring wells (HE-31 HE-48, and HE-44, each shown in red) are located within 2 km down gradient from this injection well. Major faults and their relative movements are shown in yellow as well as the location of wells at the surface (blue and red dots).

The acid gases injected into the CarbFix2 system originated from the Hellisheiði power plant. This power plant is located in SW Iceland, 25 km east of Reykjavík, the

Icelandic capital (Fig. 1). This power plant annually emits 50,000 tons of a geothermal gas mixture with a composition of 63 vol% CO_2, 21 vol% H_2S, 14 vol% H_2 and 2 vol% of other gases, predominantly N_2, Ar, and CH_4. A CO_2 and H_2S dominated gas mixture was captured from this power plant exhaust gas stream by its dissolution into pure water in a scrubbing tower (Aradottir et al., 2015; Fig. 2, Tables 1 and 2). In total, 30 to 36 kg/s of pure water is sprayed into the top of the scrubbing tower, operated at an absolute pressure of 6 bars at 20°C. This water interacts with a 0.336 m^3/s exhaust gas stream dissolving the water-soluble gases. The non-dissolved gases are vented into the atmosphere. The average composition of the water leaving the scrubbing tower contained 102 *mM* dissolved inorganic carbon (DIC) and 72.9 *mM* dissolved sulfur (Table 2), and it had a pH ranging between 3.5 and 4. The scrubbing tower is currently optimized to recover 56% of the CO_2 and 97% of the H_2S from the exhaust stream. The percentage CO_2 recovered could be increased by increasing the water to exhaust gas ratio, and/or the pressure in the scrubbing tower. A thermally stable inert tracer, 1-naftalenesulfonic acid (1-ns), was added to the gas-charged water using a dosing pump to monitor the fate of the dissolved gases after their injection. Prior to its transport from the capture plant, the resulting gas-charged water was pressurized to 9 bars.

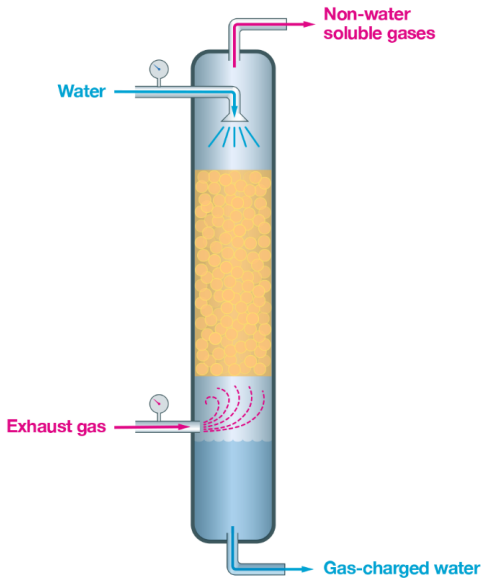

Fig. 2. Schematic illustration of the scrubbing tower in the gas capture plant. The scrubbing tower is 12.5 m high and 1 m wide and is used to capture CO_2 and other water-soluble gases. Nearly pure condensate water is injected into the top of the scrubber at 6 bars pressure and 20°C. This water flows downwards and interacts with up flowing exhaust gas at this pressure while passing through a tortuous path around the filling material (total internal volume = 4.7 m^3) within the scrubber. Remaining non-dissolved gases are vented at the top of the unit and gas-charged water leaves the scrubbing tower from the bottom.

Table 1. Average compositon and flow of gases before and after the scrubbing tower and precentage dissolved in the scrubbing unit

Gas composition	CO_2 (vol%)	H_2S (vol%)	H_2 (vol%)	N_2 (vol%)	O_2 (vol%)	CH_4 (vol%)	
Before scrubbing tower	54.5	22.7	15.9	5.44	1.14	0.40	
After scrubbing tower	52.7	1.71	34.4	8.72	1.64	0.83	
Gas flow[b]	CO_2 (m^3/s)	H_2S (m^3/s)	H_2 (m^3/s)	N_2 (m^3/s)	O_2 (m^3/s)	CH_4 (m^3/s)	Total flow (m^3/s)
Before scrubbing tower	0.183	0.0764	0.0535	0.0183	0.00383	0.00135	0.336[c]
After scrubbing tower[d]	0.0811	0.0026	0.0530	0.0134	0.00252	0.00128	0.154
	CO_2	H_2S	H_2	N_2	O_2	CH_4	
Percentage dissolved	55.8%	96.6%	1.0%	26.7%	34.2%	5.1%	

[a] Compositions and fluxes reflect conditions in the scrubber tower before the up-scale in June 2016
[b] at 1.013 bar-a and 40°C
[c] according to gas compressor specification
[d] calculated assuming 1% loss of H_2 in the scrubbing water which is in good agreement with scrubbing tower design

158

Table 2. Composition of gas charged injection water

Date	DIC (*mM*)	DS[a] (*mM*)
8.7.2014	117	71.8
11.7.2014	99.1	67.1
25.9.2014	107	74.0
16.10.2014	101	75.3
21.10.2014	93.7	70.3
4.12.2014	96.4	73.2
19.12.2014	97.9	78.3
16.1.2015	94.6	82.8
18.3.2015	81.3	71.4
13.4.2015	102	55.5
15.4.2015	102	76.4
13.5.2015	102	75.3
1.6.2015	108	67.8
30.7.2015	119	70.4
4.11.2015	107	83.4
Average	102	72.9

[a]Dissolved sulfur in the form of H_2S

159

160

161 The pressurized gas-charged water was transported via a 1.5 km long and 279 mm
162 inner diameter high density polyethylene pipe to the HN-16 injection well, where it was
163 injected into the subsurface. The injection rate was 30 to 36 kg/s, such that a total of 14.5
164 tons CO_2 and 7.9 tons H_2S were injected each day (Figs. 2 and 3). This injection well was
165 directionally drilled, 2206 m long and 0.311 m wide. The top 660 m is cased with carbon
166 steel. As the gas-charged water is acidic and corrosive to the carbon steel, this water is
167 piped to a depth of 750 m through a 4" stainless steel pipe. This prevents any contact
168 between the carbon steel and the gas-charged water. Effluent water was injected into the
169 well between the inner stainless steel pipe and the casing (Fig. 3). The effluent water had
170 a temperature ranging from 55 to 140°C, had an average pH of 9.13 (Table 3) and was

injected at a rate of 15 to 130 kg/s (Fig. 4). The two fluids, gas-charged condensate water and effluent water, mix at the exit of the stainless steel pipe at 750 m. The pH of the gas charged-effluent water mixture was calculated, using PHREEQC version 3 (Parkhurst and Appello, 2013) together with the core10 database (Neveu et al., 2017) to be ~5 at a temperature of 65 ^{o}C increasing to ~6 as its temperature increased to 250 ^{o}C. The main aquifer receiving the water mixture is located at a depth between 1900 and 2200 m. The formation temperature at the depth of this aquifer prior to injection was estimated to be 240-250°C, based on measurements from adjacent wells. Although the mildly acidic injection water could liberate potentially toxic metals to the fluid phase, we observed negligible changes to the concentrations of such metals in our sampled monitoring fluids.

The gas injection began during June 2014 and was terminated 15 July 2015. In total, 4526 tons of water dissolved CO_2 and 2530 tons of water dissolved H_2S had been injected. The fluid mass in the geothermal system does not build up over time as fluid is continuously removed from this system to provide water and steam for the powerplant. The injected gas-charged water will tend to sink once it arrives in the reservoir because 1) the injected fluid is relatively cool and 2) it is gas-rich. Both factors increase the density of the injected fluid relative to that of the hot dilute formation water (e.g. Patel and Eubank, 1988; Teng et al., 1997; Hebach et al., 2004; Burton and Bryant, 2009; Pool et al., 2013). Notably, taking into account the fluid temperature and salinity, and using equations reported by Duan et al. (2008), the injected aqueous fluid has a density of 0.95 to 0.99 g/cm^3 whereas the formation fluid has a density ranging from 0.78 to 0.84 g/cm^3. This density difference, however decreases to less than 1% as the temperature of the injected fluid increases to that of the target basaltic reservoir.

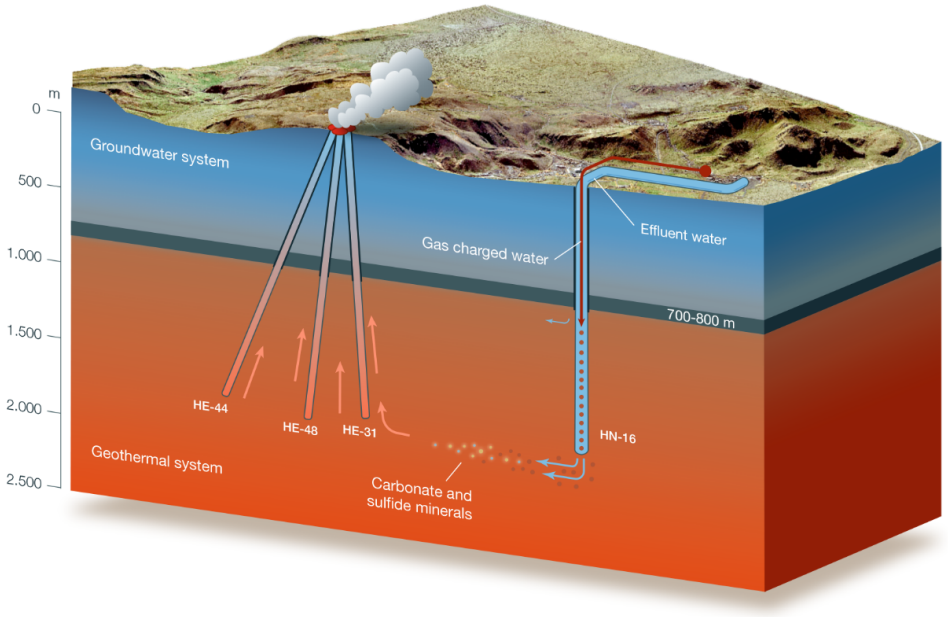

Fig. 3. Schematic cross section of the CarbFix2 injection site. Gas-charged and effluent water are injected separately to a depth of 750 m into well HN-16, then allowed to mix until they enter the aquifer at a depth of 1900 to 2200 m. This combined fluid flows down a hydraulic pressure gradient to monitoring wells HE-31, HE-48, and HE-44 located 984, 1356, and 1482 m from the injection well at the reservoir depth.

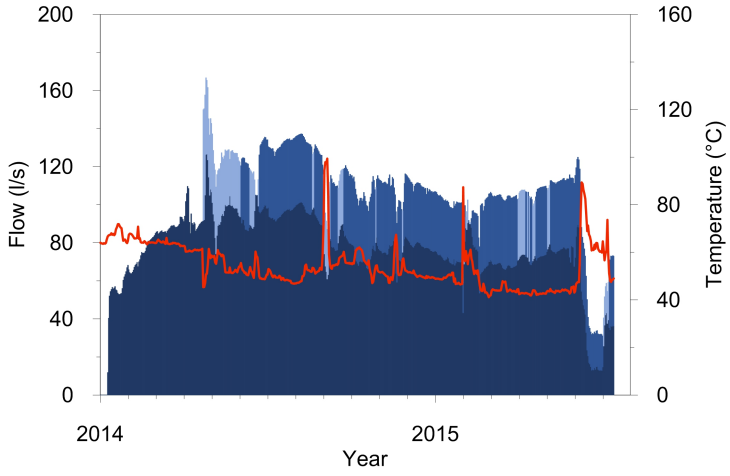

Fig. 4. Temporal evolution of the effluent water flow (dark blue area), gas-charged water flow (blue area), condensate water without gas (light blue area) and temperature of the combined fluids (red curve) in the HN-16 injection well.

208

209

Table 3. Chemical composition of effluent water from Hellisheiði power plant

Sample no	Date	pH/T (°C)	Si (*mM*)	Na (*mM*)	K (*mM*)	Ca (*mM*)	Mg (*mM*)	Fe (*mM*)	Al (*mM*)	Cl (*mM*)	F (*mM*)	DIC (*mM*)	H_2S (*mM*)	SO_4 (*mM*)
2014 - 5198	23.6.2014	9.65/23.3	8.19	6.37	0.637	0.0157	<0.002	0.004	0.049	3.37	0.057	0.398	0.432	0.358
2014 - 5240	21.7.2014	9.23/23.7	8.01	6.07	0.604	0.0164	<0.002	<0,001	0.046	3.15	0.049	0.332	0.281	0.302
2014 - 5359	1.10.2014	9.12/23.3	7.99	5.98	0.604	0.0134	<0.002	<0,001	0.046	3.30	0.051	0.453	0.367	0.261
2014 - 5376	27.10.2014	9.05/23.3	8.22	6.03	0.609	0.0132	<0.002	<0,001	0.046	3.36	0.049	0.646	0.500	0.235
2014 - 5384	3.11.2014	8.99/25.0	8.44	6.35	0.637	0.0135	<0.002	<0,001	0.049	3.58	0.051	0.351	0.487	0.239
2014 - 5398	17.11.2014	8.80/25.2	8.14	6.03	0.611	0.0124	<0.002	<0,001	0.046	3.29	0.048	0.452	0.480	0.209
2015 - 5181	4.3.2015	9.10/16.9	8.20	6.05	0.611	0.0157	<0.002	<0,001	0.047	3.47	0.051	0.339	0.550	0.121

210

211

212 *2.2 Sampling and analysis*

213 The fate of the injected gas mixture was monitored by the regular sampling of three
214 monitoring wells, located 984 m (HE-31), 1356 m (HE-48), and 1482 m (HE-44)
215 downstream from the injection well at the depths of the main aquifers, of about 1900-2200
216 m depth (Figs. 1 and 3). At these depths, the reservoir fluid is a single-phase aqueous fluid
217 with a temperature of 266 to 277 °C, as the hydrostatic pressure is greater than the liquid-
218 vapor saturation pressure of water (see supplementary material). As the fluid rises up the
219 monitoring wells, it boils as the pressure decreases. Consequently, steam and water are
220 sampled separately at 5.7 to 9.3 bars at the top of each monitoring well. Samples for the
221 determination of dissolved inorganic carbon (DIC), hydrogen sulfide (H_2S), sulfate (SO_4)
222 and the 1-ns (1-naphthalenesulfonate) tracer in the liquid phase, and CO_2, methane (CH_4)
223 and H_2S in the vapor phase were collected using a Webre separator. The sampling
224 procedure for these samples is described in detail by Arnórsson et al. (2006).

225 Distinct methods were used to measure the concentrations of the dissolved gases in
226 the sampled fluids. The procedure used for the analysis of CO_2 and H_2S in the vapor phase
227 as well as DIC and sulfide in the liquid phase is described in Arnórsson et al. (2006). The

228 H_2S in the vapor phase, after its dissolution into a NaOH rich aqueous solution, was
229 analyzed by titration with silver nitrate and silver electrode endpoint detection (Metrohm
230 905 Titrando). The CH_4 in the vapor phase together, with other major geothermal gases,
231 were analyzed using an Agilent Technologies 7890A gas chromatography system using a
232 HP-Molesieve (19095P-MSO) column and Thermal Conductivity Detector. Subsamples
233 collected for aqueous sulfate concentration determination, previously treated at the
234 sampling site with Zn acetate to precipitate sulfide as zinc sulfide preventing H_2S oxidation
235 to SO_4 upon storage, were filtered through 0.2 μm cellulose acetate filters in the laboratory
236 and subsequently analyzed using a Dionex ICS-2000 chromatography system. Samples for
237 1-ns tracer measurements were filtered through 0.2 μm cellulose acetate filters into 60 ml
238 amber glass bottles and analyzed using a Thermo Ultimate 3000 HPLC with a BetaBasic
239 C-18 column and fluorimetric detection. The analytical method adopted for these analyses
240 was based on that described by Rose et al. (2002), but with a 100 mm column and a
241 gradually increasing MeOH concentration in the eluent. The detection limit for 1-ns is
242 $5x10^{-7}$ *mM*. Measured concentrations for DIC, H_2S and SO_4^{-2} in liquid phase samples and
243 for CO_2, H_2S and CH_4 in vapor phase samples are orders of magnitudes higher than the
244 detection limits of the analytical methods.

245

246 *2.3 Calculation of reservoir fluid compositions and fraction mineralized*

247 Concentrations of DIC, CH_4, H_2S, SO_4 and 1-ns in the sampled reservoir fluids
248 before phase separation were calculated using the WATCH speciation program (Arnórsson
249 et al., 1982; Bjarnason, 2010) from the analyzed concentration in the liquid and vapor
250 phase, and the vapor fraction at collection pressure using:

$$m_i^{f,t} = m_i^{d,l}\left(1 - X^{d,v}\right) + m_i^{d,v} X^{d,v} \quad (1)$$

where m_i designates concentration of the component i, d stands for discharge, t for total, f for fluid, l and v for liquid and vapor. The $X^{d,v}$ stands for the vapor fraction at the sampling pressure. The concentration of 1-ns and SO_4 was assumed to be zero in the vapor phase and the concentration of CH_4 was assumed to be zero in the liquid phase. The pH at the reservoir temperature was calculated from measured pH value of the water phase at ambient temperature and the major element composition of the water and steam phase using the WATCH speciation program (Arnórsson et al., 1982; Bjarnason, 2010).

The HE-31, HE-48, and HE-44 monitoring wells are liquid enthalpy wells meaning that their discharge enthalpy corresponds closely to the enthalpy of the single-phase reservoir fluid at the reservoir temperature. The vapor fraction at the sample collection pressure was therefore calculated assuming adiabatic boiling from the reservoir temperature to the sampling pressure (c.f. Arnórsson et al., 2007). The reservoir temperature was calculated assuming equilibrium with quartz (Gunnarsson and Arnórsson, 2000) to be 266 °C for wells HE-31 and HE-48 and at 277°C for well HE-44. These temperatures agree well with the measured temperature at the depth of the aquifers in the wells.

The concentrations of dissolved sulfur (DS) in the reservoir fluid $\left(m_{DS}^{f,t}\right)$ were calculated from the concentration of H_2S $\left(m_{H_2S}^{f,t}\right)$ and SO_4^{2-} $\left(m_{SO_4}^{f,t}\right)$ in the reservoir fluid using:

$$m_{DS}^{f,t} = m_{H_2S}^{f,t} + m_{SO_4}^{f,t} \quad (2)$$

The total amount of gas injected during this study was a mixture of 4526 tons CO_2 and 2530 tons H_2S. This amount was calculated based on the flow of gas-charged water into the injection well and the concentration these gases in the water. A total of 405 kg of the 1-ns tracer were injected over this same period. The tracer-bearing aqueous solution was prepared in batches of one cubic meter at a time. One hundred kg of 1-ns sodium salt (1-naphthalenesulfonic acid sodium salt, CAS no: 130-14-3, molecular weight 230.22 g/mole) was dissolved in 1000 kg water and injected at a constant proportion to the gas-charged water using a Milton Roy dosing pump. The molar ratio between the DIC and DS, and the 1-ns tracer was 81270 and 58880, respectively.

Following the approach of Matter et al. (2016), the fraction of the injected gas mineralization was computed by comparing measured aqueous DIC and DS concentrations in the sampled monitoring wells to those calculated assuming no reactions occurred in the subsurface. Concentrations of DIC and DS, assuming only the unreactive mixing of fluids ($m^{f.t}_{DIC,predicted}$ and $m^{f.t}_{DS,predicted}$), were determined from the measured concentrations of the injected non-reactive tracers using:

$$m^{f,t}_{i,predicted} = m^{f,t}_{i,background} + \left(m^{f,t}_{1-ns} - m^{f,t}_{1-ns,background}\right)A \quad (3)$$

where *A* designates the molar ratio between the DIC or DS and tracer in the gas-charged injection water. The background concentrations of DIC and DS in the monitoring wells were calculated by averaging selected DIC and DS concentrations in the initial reservoir fluid before the arrival of gas-charged injection water to the monitoring wells (Table 4). The background concentration for DIC was calculated to be 8.36 *mM*, 9.82 *mM*, and 18.1 *mM* in monitoring wells HE-31, HE-48 and HE-44. The corresponding values for DS were

1.27 *mM*, 1.38 *mM*, and 2.11 *mM* for wells HE-31, HE-48, and HE-44. The background concentration of 1-ns present in the geothermal system originates from the breakdown of other sulfonates used in previous tracer tests of the geothermal reservoir at Hellisheiði (Kristjánsson et al., 2016). The background concentration in the reservoir fluid $\left(m^{f,t}_{1-ns,background}\right)$ in wells HE-31, HE-48, and HE-44 was 6.95x10^{-7} *mM*. Comparison of the observed and predicted DIC and DS concentrations in the monitoring wells allows for the calculation of fraction of gases mineralized in the subsurface. The fraction mineralized is calculated using the equation:

$$Fraction\,Mineralized = \frac{\left(m^{f,t}_{i,predicted} - m^{f,t}_{i}\right)}{\left(m^{f,t}_{i,predicted} - m^{f,t}_{i,background}\right)} \quad (4)$$

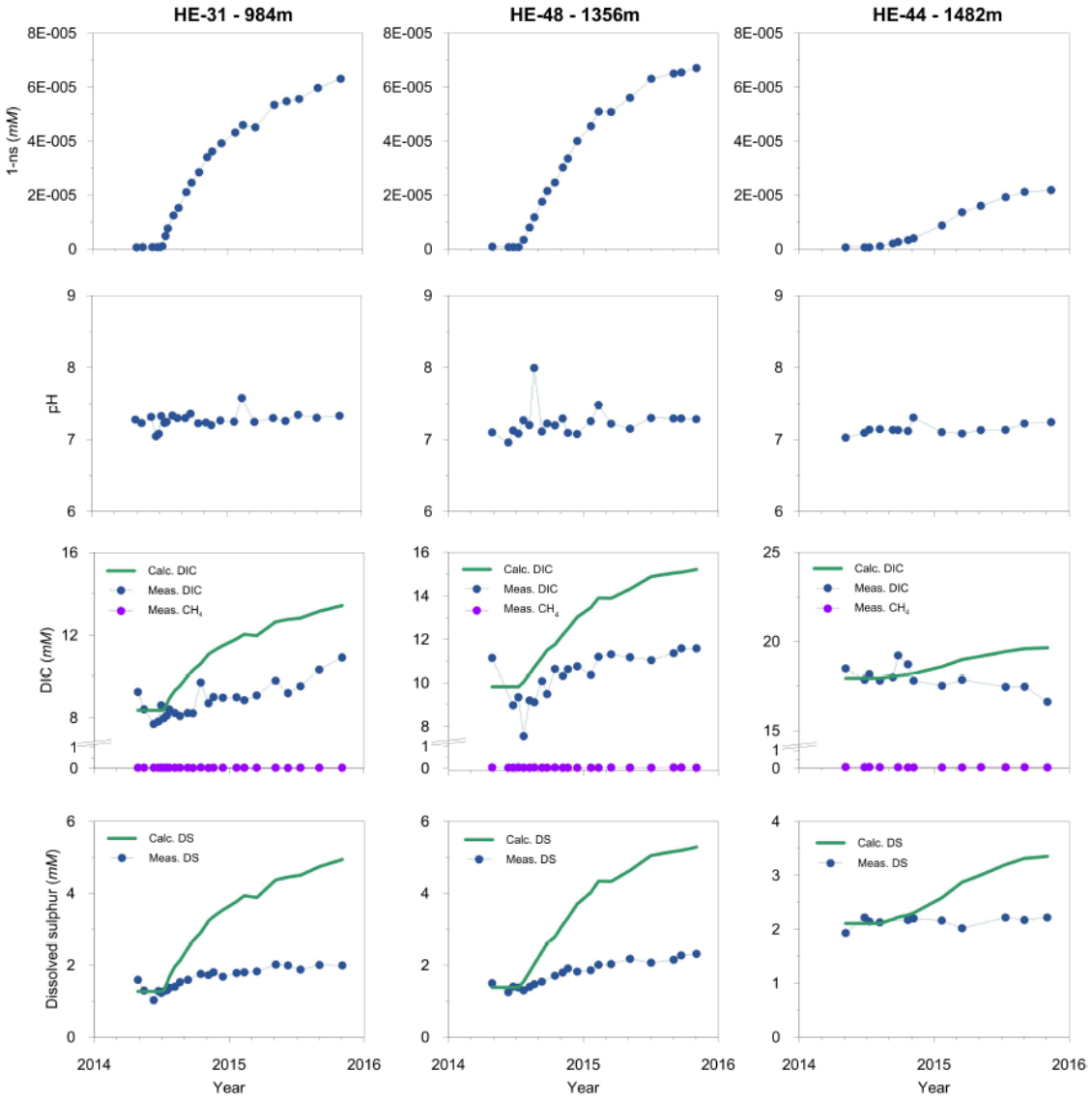

Fig. 5. The temporal chemical evolution of water samples collected from the HE-31, HE-48 and HE-44 monitoring wells located 984, 1356, and 1482 m, respectively, from the HN-16 injection well as indicated in the column headings. The top row of plots illustrates the measured dissolved 1-naftalenesulfonic acid (1-ns) tracer concentration. The second row of plots show the calculated pH of the sampled fluids at reservoir temperature. The third row of plots show the measured and calculated concentrations of dissolved inorganic carbon (DIC) and methane. The bottom row of plots depicts the measured and calculated total dissolved sulfur concentration (DS). Calculated values shown by the green lines were generated assuming only dilution and mixing affected the fluid compositions and the measured values of 1-ns, DIC and DS are shown as filled blue circles. The filled violet circles in the plots correspond to measured methane

concentrations. The difference between the green and blue lines correspond to that fixed by chemical reactions occurring in the reservoir.

3. Results

The total measured dissolved inorganic carbon (DIC), methane (CH_4), total dissolved sulfur (DS), pH at 25 °C, and 1-ns tracer concentrations in the monitoring wells HE-31, HE-48 and HE-44 (Fig. 5) are listed in Table S-1. The first appearance of the 1-ns tracer was observed 17, 32, and 47 days after the beginning of the injection in wells HE-31, HE-48, and HE-44, respectively (Fig. 5). Due to subsurface mixing and dispersion, the average time for the tracer to flow from the injection well to monitoring wells HE-31, HE-48, and HE-44 (Fig. 2) is greater and determined to be 130, 163, and 272 days, respectively (Kristjánsson et al., 2016). The tracer concentrations in the monitoring well fluids continue to increase at the end of the study period as the flow system had not yet attained a steady-state concentration in response to the continuous injection of dissolved gases and tracer.

The fate of the injected gases was quantified using mass balance equations (3) and (4). Results of these calculations, providing estimates of what the concentrations of DIC and DS in the sampled monitoring well fluids would be in the absence of chemical reactions, are listed in Table S-1 and shown in Fig. 5. These calculated values are substantially higher than those measured in these monitoring wells, suggesting a loss of DIC and DS along the subsurface flow path towards the monitoring wells. The only plausible mechanism for this difference is carbon- and sulfur-bearing mineral precipitation. The difference between the calculated and measured DIC and DS suggests that over 50% of the injected CO_2 and 76% of the injected H_2S were mineralized through water-gas-basalt interaction during the 130 to 272 days required for its transport from the injection to the

monitoring wells (Table S-1, Fraction mineralized). Similar observations demonstrated the mineralization of injected CO_2 and H_2S during the original CarbFix project within two years at 20-50°C (Matter et al., 2016; Snæbjörnsdóttir et al., 2017). Once mineralized, the risk of gas leakage to the surface is eliminated and a monitoring program of the storage site can be significantly reduced, thus enhancing storage security and potentially public acceptance.

An additional observation is that the permeability of the injection well was stable throughout the injection (Fig. 4), suggesting the long-term viability of these wells and this carbon storage approach. This later observation is consistent with the relatively low pH of the injected gas-charged injection water, which was undersaturated with respect to calcite, and most of the minerals present in the aquifer rocks.

4. Discussion

4.1 Injected gas mineralization and permeability

A significant result of this study is that the permeability of the target injection reservoir remained stable throughout the two-year injection despite the successful mineralization of much of the injected gases, likely as calcite and pyrite. There are two major reasons for this. First, the injected gas-charged fluids are acidic so that they are strongly undersaturated with respect to the basalts in the target aquifer. The undersaturation of this fluid leads to the dissolution of the host rock basalts in the vicinity of the injection well. Significant mineralization will only occur at a distance away from the injection well

365 after heat exchange and sufficient dissolution of the host rock neutralizes the gas-charged
366 water and saturates the formation water with respect to carbonate and sulfur minerals.

367 The second major reason for the stable permeability of the target reservoir over the
368 2-year injection period is likely the relatively small amount of mineral reaction compared
369 to the size of the reservoir. The volume of calcite created by the mineral storage of one ton
370 of CO_2 is 0.84 m^3; the volume of pyrite created by the mineral storage of one ton of H_2S is
371 0.70 m^3. As such, the total volume of calcite and pyrite created if all the gas injected
372 during this study formed these minerals would be 5,560 m^3. This compares to a reservoir
373 volume of $6x10^8$ m^3, determined assuming the target reservoir was 200 m in height, 200 m
374 in width, and 1500 m in length. The volume of the precipitated calcite and pyrite would
375 thus constitute only 0.009 volume percent of the reservoir. This compares with an
376 estimated 8 to 10% porosity of the target reservoir basalts (Gunnarsson et al., 2011). The
377 degree to which longer-term and or larger gas injections will alter permeability over time
378 cannot be assessed at present, but it should be noted that the carbonation of basalts is a
379 complex set of reactions that involve the dissolution of the host basalts and the potential
380 precipitation of a large number of secondary phases in addition to calcite and pyrite (Gysi
381 and Stefansson, 2011; Gysi, 2017, Snæbjörnsdóttir et al., 2018). Moreover, the relationship
382 between permeability and porosity, mineral dissolution, and mineral precipitation is
383 complex and poorly understood at present (c.f.. Oelkers 1996; Jove et al., 2004; Nogues et
384 al., 2013; Noirel et al., 2016; Beckingham, 2017). As such the long-term effect of this
385 carbon and sulfur geologic storage approach might be best studied directly as long-term
386 industrial-scale acid gas subsurface injection projects.

387

388 *4.2 The cost of the described CCS approach*

389 A major advantage of the CCS approach described above is its cost and safety
390 relative to conventional technologies. The capture does not involve the separation of a pure
391 and dry CO_2 phase; it captures all water-soluble gases in a single step by its dissolution
392 into water, which is then directly injected into the subsurface at 9 bars absolute pressure.
393 As a result, only water and electricity is needed for capture. The overall "on site cost" of
394 this gas mixture capture, transport and storage at the CarbFix2 Hellisheiði site is US
395 $24.8/ton (Fig. 6 and Table 4).

396

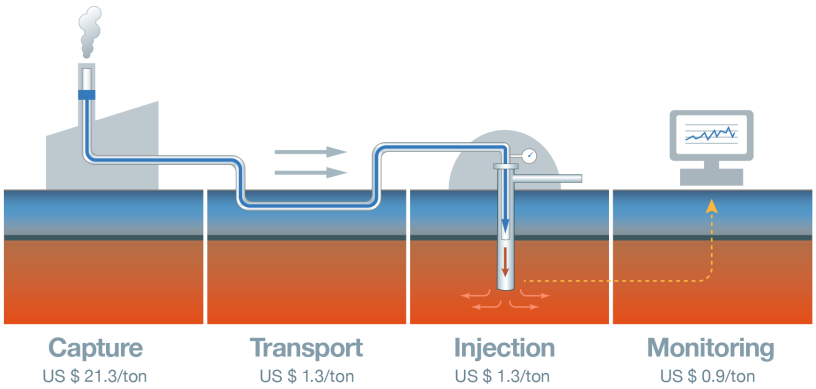

397

398 *Fig. 6. Schematic illustration of the running cost of this integrated CCS solution at the*
399 *CarbFix2 site. Costs are given in US$ per ton of gas mixture (CO_2 + H_2S) injected and*
400 *assume "on- site" existing infrastructure, electricity cost and transport distance of 1.5*
401 *km as detailed in the text.*

402

403

404

Table 4. Cost of mixed gas capture (CO_2 + H_2S) and storage at the CarbFix2 site

	Case 1[a] (US $/ton)	Case 2[b] (US $/ton)	Case 3[c] (US $/ton)
Capture	21,3	21,3	42,1
Transport	1,3	1,3	1,3
Injection	1,3	4,1	4,1
Monitoring	0,9	0,9	0,9
Total CCS cost	24,8	27,6	48,4

[a] on site up-scaled cost at Hellisheiði power plant

[b] on site up-scaled cost at Hellisheiði power plant including drilling a well for injection

[c] on site up-scaled cost at Hellisheiði power plant including drilling a well and using average OECD electricity price for industry in 2014 (US $ 123,9 /MWh) (IEA, 2016)

These cost calculations were based on "on-site" necessary capital expenditure (CapEx) and operating costs for capture, transport, injection, and monitoring, levelized to the total amount of gas injected for the time period in this study and assuming ISK/USD exchange rate of 130. All equipment and infrastructure were assumed to have a lifetime of 30 years and relevant cash flow projected for each year. Annual deprecation for property, plant and equipment (PP&E) were assumed to be 3% and the effective tax rate 20%. Total cost per ton of mixed gas captured and injected over the 30-year lifetime was calculated by using the equivalent annual cost (EAC), where annual capture and injection rates were assumed to remain fixed at the current "up-scaled" capacity with 24 hour year-round operation, apart from a two week annual maintenance stop. Lower tax payments due to operational losses for the project were considered as a revenue stream in the project's cash flow.

This overall up-scaled cost is dominated by that of gas mixture capture estimated to cost US $21.3/ton; a considerable part of this capture cost stems from compressing the gas and pure water to 6 bars and then further pressurizing the resulting gas-charged water

to 9 bars prior to injection (Figs. 2 and 6). Note that this capture method also has the advantage of not using organic absorbents or solvents, such that it has less potential environmental influence. The on-site, up-scaled cost of transport and injection of the gas-charged fluid into the injection well is US $1.3/ton and US $1.3/ton, respectively; the bulk of this cost originates from the building of the additional infrastructure at the Hellisheiði site. The cost of injection, estimated here, excludes the drilling costs of the pre-existing wells at the CarbFix2 site. Estimates (Table 4) show that including the cost of drilling a suitable gas injection well at Hellisheiði would increase the cost of injection from US $1.3/ton to US $3.1-5.0/ton, depending on the depth of the well. The average of this additional cost is shown in Table 4. The cost of monitoring, estimated at US $0.9/ton, includes four soil gas flux measurements, injectivity, P-T, spinner and downhole camera measurements every five years, as well as bi-monthly sampling of the monitoring wells for five years after the start of injection and thereafter twice a year for the remaining 25 years of the estimated duration of this injection.

The pipe that transports the gas charged water towards the injection well (Fig. 1), located at approximately 1.5 km distance from the power plant, is buried 1 m in the ground and only 1% of the total mass it transports is CO_2 and H_2S. The transport of the gas as a dissolved phase in condensate water elevates the cost significantly compared to conventional gas transport, where it is only necessary to transport pure dry gas. When settings require further transport of gas to injection sites, the cost of transport could be brought down by adding a degassing step after the gas scrubbing tower. The CO_2 gas could then be transported in smaller and lower grade pipes above surface, as the risk of water

444 freezing of this anhydrous gas would be minimal. The CO_2 could then be re-dissolved in
445 water at the injection site before or during injection.

446

447 *4.3 Potential cost of this CCS approach at other sites*

448 The overall cost and efficiency of the CCS approach described in this study will
449 differ depending on the site, depth of injection well, composition of the exhaust gas to be
450 treated, and the price of the energy used to capture the acid gases from the exhaust stream.
451 Although it is not possible to consider all of these factors in estimating the costs of this
452 CCS approach at other sites, it is possible to evaluate the effects of different energy costs
453 and of a need to drill an injection well on the overall costs. Note that the "on site costs" of
454 transport, injection and monitoring are not affected by the electricity price, only that of the
455 acid gas capture.

456 The overall CCS cost at the CarbFix2 site based on three cost scenarios for a 1.5
457 km transport of gas mixture; 1) "on-site conditions", 2) adding the cost of a new injection
458 well, and 3) taking account the cost of new injection well and average OECD electricity
459 price for industry in 2014 (IEA, 2016), is shown in Table 4. The three CCS cost estimates
460 reported in Table 4, which range from US $25/ton to US $50/ton, are generally lower than
461 cost estimates for conventional pure and dry CO_2 capture and storage (CCS), which range
462 from US $38 to US $143/ton CO_2 (Global CCS Institute, 2011; Rubin et al., 2015). Our
463 estimated CCS costs are also somewhat lower on average than the US $35 to US $65/ton
464 recently estimated as the CCS cost at Chinese coal fire power plants (Hu and Zhai, 2017).
465 The exact cost of adopting this CarbFix approach will vary site to site depending on a
466 number of factors including gas composition, depth of target storage reservoir, and local

energy costs (c.f. Rubin et al., 2015). The CCS costs using this CarbFix approach, however, would be offset by the co-fixation of sulfur through this process. As sulfur capture and storage can exceed US $300/ton (U.S. Department of Energy, 2013), this integrated method may provide the financial incentive for the general application of capturing and injecting water-soluble gas mixtures into reactive rocks.

The capture and storage of the mixed CO_2-H_2S gas at the Hellisheiði power plant using this CarbFix method may be particularly favorable compared to other sites due to the availability of a CO_2-rich gas stream, local permeable basalts, and abundant fresh water. The degree to which this or a similar approach will prove economically viable at other sites depends to a large extent on the composition of the exhaust gas and identity of the subsurface rock formations. The efficiency of CO_2 capture with other water-soluble gases in water diminishes with the decreasing CO_2 content of the exhaust gas. Consequently, the efficient capture of CO_2 and other water-soluble gases could require higher pressures in the scrubber for exhaust streams that are less concentrated in CO_2. This would increase capture costs, as these costs are dominated by the cost of pressurizing the exhaust gas-water stream. As the cost of capture is directly related to the pressure required in the scrubber, the optimization of scrubber pressure and water demand will need to be considered on a site by site basis.

There are many places around the world, however, which have both abundant water and permeable basalts, which may provide conditions for the further application of this CCS approach. Notably, the ocean floor is comprised mostly of basalts and adjacent to an inexhaustible supply of seawater (McGrail et al., 2006; Goldberg et al., 2008; Wolff-Boenisch, 2011; Gislason and Oelkers, 2014; Snæbjörnsdóttir et al., 2014), which may

490 make the CCS methods described above favorable along many continental coastlines and
491 on volcanic islands. For example, the subseafloor basalts of the Juan de Fuca ridge off the
492 coast of the Pacific northwest of the United States have been reported to have porosities of
493 >10%, premeabilites estimated to range from 10^{-9} to 10^{-5} cm^2, and a potential pore volume
494 of 780 km^3 (Goldberg et al., 2008). These authors concluded that this formation alone
495 could store ~250 Gt of carbon as calcite. Moreover, the subsurface storage capacity of the
496 porous basaltic rocks in Iceland has been estimated to be up to ~2500 Gt of CO_2
497 (Snæbjörnsdóttir et al., 2014), which is approximately 25 times that required prior to 2050
498 as part of an integrated effort to limit global warming to 2°C (IEA, 2015). In addition,
499 seawater is commonly used in flue gas desulfuration (FGD), where seawater cooled fossil
500 fueled power plants use the seawater to scrub sulfur dioxide from flue gas (Olkawa et al.,
501 2003). The application of the CarbFix approach to will, however, need to account 1) for
502 the lower solubility of CO_2 in seawater compared to that of fresh water; CO_2 is
503 approximately 15% less soluble in seawater depending on the temperature and pressure
504 (Weiss, 1974), and 2) the additional costs associated with the transport of gas to the coast
505 for subseafloor injection. The mineralization of CO_2 charged seawater may be somewhat
506 accelerated as the dissolution rates of basalt are somewhat enhanced in CO_2-charged
507 seawater compared to CO_2-charged fresh water (Wolff-Boenisch et al., 2011). This more
508 rapid basalt dissolution, likely does not lead to secondary mineral precipitation at
509 temperatures less than 150 ^oC dissolution, as like its freshwater equivalent, CO_2-charged
510 seawater is strongly undersaturated with respect to precipitating phases at these conditions.
511 Note, however, that at temperatures in excess of 150 ^oC, anhydrite precipitation from
512 injected seawater would be favored (Bischoff and Seyfried, 1978). The precipitation of

513 anhydrite from the heating of CO_2-charged seawater as it is injected to high temperature
514 basalts could pose a threat to the long-term injectivity of an injection well.

515

516 *4.3 Carbon storage and waste water disposal*

517 A critical factor in the application of this CarbFix approach for storing carbon by
518 its mineralization in reactive rocks is the ability to inject large volumes of water into the
519 subsurface. At a pressure of 25 bars, approximately 27 tons of pure water at 25°C are
520 required to dissolve each ton of CO_2 gas prior to or during its injection (Gislason et al.,
521 2010; 2014). Large volumes of effluent water are, however, being injected into subsurface.
522 There are currently 20-25 million tons of effluent water being injected into the subsurface
523 basalts at Hellisheiði each year (Reykjavík Energy, 2016), sufficient for the dissolution and
524 injection of close to one million tons of acid gases annually, or roughly 20 times the CO_2
525 emitted at Hellisheiði power plant. The amount of waste and effluent water injected
526 annually into the subsurface through industrial processes is far larger. It has been estimated
527 that more than 3 Gt/y of oil field brines are brought to the surface in US and UK alone
528 (American Petroleum Institute, 2000; UK Oil and Gas Industry Association, 2016).
529 Reinjection is the primary disposal method. As such this may provide an opportunity to
530 adopt some of the technology developed by this CarbFix method at other sites.

531

532 **5. Conclusions**

533 This study has demonstrated the efficiency and cost advantages of the capture and
534 storage of mixed gas streams at the CarbFix2 site. Typical coal-fired power plant exhaust

contains substantial quantities of oxidized sulfur and nitrogen gases, which are highly soluble in water (Freund et al., 2005). The simultaneous capture and storage of these gases with CO_2 may provide an additional economic incentive to make this CCS method a valuable contributor to the global effort to limit the increasing carbon concentration of the atmosphere.

The CCS approach described above also has the advantage of enhanced safety; the injected gas-charged water is less buoyant than the formation water, leading it to sink once injected into the subsurface. Moreover, this injection provokes the fast subsurface mineralization of much of the injected acid gases over month long time frames. As such, if it is possible to adapt this approach at other sites, its increased storage security may both lower monitoring costs and enhance public acceptance of CCS at other locations throughout the world.

Acknowledgments- We acknowledge funding from Reykjavik Energy; the European Commission through the projects CarbFix (EC coordinated action 283148), Min-GRO (MC-RTN-35488), Delta-Min (PITN-GA-2008-215360), and CO2-REACT (EC Project 317235) to S.R.G., E.H.O., and Reykjavik Energy; CarbFix2 (European Union's Horizon 2020 research and innovation programme under grant number 764760); S4CE (European Union's Horizon 2020 research and innovation programme under grant number 764810); Nordic fund 11029-NORDICCS; the Icelandic GEORG Geothermal Research fund (09-02-001) to S.R.G. and Reykjavik Energy; and the U.S. Department of Energy under award number DE-FE0004847 to J.M.M and M.S.; We thank Þ. A. Þorgeirsson , T. Kristinsson, H. Bergmann, S. S. Sigurðardóttir, V. Eiríksdóttir, C. Marieni and F. Jónsdóttir for helping with sample collection in the field and analysis.

References

American Petroleum Institute, 2000. Overview of Exploration and Production Waste Management Volumes and Waste Management Practices in the United States.

565 American Petroleum Institute. http://www.api.org/environment-health-and-
566 safety/environmentalperformance/~/media/Files/EHS/Environmental_Performance/I
567 CF-Waste-Survey-of-EandP-Wastes-2000.ashx

568 Alfredsson, H.A., Oelkers, E.H., Hardarsson, B.S., Franzson, H., Gunnlaugsson, E. and
569 Gislason, S.R., 2013. The geology and water chemistry of the Hellisheidi, SW-Iceland
570 carbon storage site. Int. J. Greenh. Gas Control 12, 399-418.

571 Aradottir, E.S.P., Gunnarsson, I., Sigfusson, B., Gunnarsson, G., Juliusson, B.M.,
572 Gunnlaugsson, E., Sigurdardottir, H., Arnarson, M.T., Sonnenthal, E., 2015 Toward
573 cleaner geothrnel energy utilization: Capturing and sequestering CO_2 and H_2S
574 emissions from geothermal power plants. Transport in Porous Media 108, 61-84.

575 Arnórsson, S., Bjarnason, J. Ö., Giroud, N., Gunnarsson, I., Stefansson, A., 2006. Sampling
576 and analysis of geothermal fluids. Geofluids 6, 203–216.

577 Arnórsson, S., Stefánsson, A., Bjarnason, J.Ö., 2007. Fluid–fluid interactions in
578 geothermal systems. Rev. Min. Geochem. 65, 259–312.

579 Arnórsson, S., Sigurdsson, S., Svavarsson, H., 1982. The chemistry of geothermal waters
580 in Iceland. 1. Calculation of aqueous speciation from 0°C to 370°C. Geochim.
581 Cosmochim. Acta 46, 1513-1532.

582 Benson, S.M., Cook, P., Coordinating Lead Authors. Anderson, J., Bachu, S., Nimir, H.B.,
583 Basu, B., Bradshaw, J., Deguchi, G., Gale, J., von Goerne, G., Heidug, W., Holloway,
584 S., Kamal, R., Keith, D., Lloyd, P., Rocha, P., Senior, B., Thomson, J., Torp, T.,
585 Wildenborg, T., Wilson, M., Zarlenga, F., Zhou, D, Lead Authors. Celia, S.M., Gunter,
586 B., Ennis King, J., Lindegerg, E., Lombardi, S., Oldenburg, C., Pruess, K., Rigg, A.,
587 Stevens, S., Wilson, E., Whittaker, S., 2005. Underground Geological Storage, IPCC
588 Special Report on Carbon Dioxide Capture and Storage, Chapter 5. Intergovernmental
589 Panel on Climate Change, Cambridge University Press, Cambridge, U.K.

590 Bischoff J. L., Seyfried W. E. Jr., 1978. Hydrothermal chemistry of seawater from 25 °
591 to 350°C. Ame. J, Sci. 278, 838–860.

592 Bjarnason, J. Ö. 2010. The chemical speciation program WATCH, version 2.4. *ISOR –*
593 *Iceland Geosurvey*, Reykjavík, Iceland.
594 http://www.geothermal.is/sites/geothermal.is/files/download/watch_readme.pdf

595 Blount, G., Gorensek, M., Hamm, L., O'Neil, K., Kervevan, C., 2017. CO_2 dissolved and
596 aqueous gas separation. Energy Procedia, 114**,** 2675-2681.

597 Beckingham, L.E., 2017. Evaluation of macroscopic porosity-permeability relationships in
598 heterogeneous mineral dissolution and precipitation scenarios. Water Resources Res.
599 53, 10217-10230.

600 Burton, M., and Bryant, S.L., 2009. Eliminating buoyant migration of sequestered CO_2
601 through surface dissolution: Implementation costs and technical challenges. SPE
602 Reservoir Evaluation and Engineering 12, 399-407.

603 Duan, Z., Hu, J., Li, D., Mao, S. 2008. Densities of the CO_2-H_2O and CO_2-H_2O-NaCl
604 systems up to 647 K and 100 MPa.Energy & Fuels 22, 1666-1674.

605 Franzson H., 1988. Nesjavellir: Permability in geothermal reservoir" (in Icelandic) OS-
606 88046/JHD-09, Energy Authorities of Iceland, Reykjavik.

607 Franzson, H., Gunnlaugsson, E., Árnason, K., Sæmundsson, K., Steingrímsson, B.
608 Harðarson, B., 2010. Hengill geothermal system, conceptual model and thermal
609 evolution. *Proc*. World Geothermal Congress 2010.

610 Franzson H., Kristjansson, B.R., Gunnarsson, G., Björnsson, G. Hjartarson, A.,
611 Steingrimsson, B., Gunnlaugsson, E., and Gislason, G., 2010. "The Hengill-Hellisheidi
612 Geothermal Field. Development of a Conceptual Geothermal Model" Proceedings
613 World Geothermal Congress, Antalya, Turkey.

614 Freund, P. Bachu, S., Simbeck, D. Thambimuthu, K., Gupta, M., 2005. Properties off CO_2
615 and carbon – based fuels, in *IPCC Special Report on Carbon Dioxide Capture and*
616 *Storage*. B. Metz, O. Davidson, H. Coninck, M. Loos, L. Meyer, Eds. (Cambridge
617 Univ. Press), 383-398.

618 Gerdemann, S.J., Dahlin, D.C., O'Connor W.K. 2002. Carbon dioxide sequestration by
619 aqueous mineral carbonation of magnesium silicate minerals. Proceedings of the 6th
620 international conference on Greenhouse Gas Control Technologies, Kyoto, Japaan.

621 Gislason, S.R., Broecker, W.S., Gunnlaugsson, E., Snæbjörnsdóttir, S. Ó., Mesfin, K. G.,
622 Alfredsson, H.A., Aradottir, E. S., Sigfusson, B., Gunnarsson, I. Stute, M., Matter, J.
623 M. Arnarson, M. T., Galeczka, I. M., Guðbrandsson, S., Stockman, G., Wolff-
624 Boenisch, D., Stefansson, A., Ragnheidardottir, E., Faathen, T., Gysi, A.P., Olssen, J.,
625 Didriksen, K., Stipp, S. L. S., Menez, B., Oelkers, E.H., 2014. Rapid solubility and
626 mineral storage of CO_2 in basalt. Energy Procedia 63, 4561–4574.

627 Gislason, S.R., Oelkers, E.H. 2003. Mechanism, rates, and consequences of basaltic glass
628 dissolution: II. An experimental study of the dissolution rates of basaltic glass as a
629 function of pH and temperature Geochim. Cosmochim. Acta 67,3817-3832.

630 Gislason, S.R., Oelkers, E.H., 2014. Carbon Storage in Basalt. Science 344, 373-374.

631 Gislason, S.R., Wolff-Boenisch, D., Stefansson, A., Oelkers, E.H., Gunnlaugsson, E.,
632 Sigurdardottir, H., Sigfusson, B., Broecker, W.S., Matter, J.M., Stute, M., Axelsson,
633 G., Fridriksson, T., 2010. Mineral sequestration of carbon dioxide in basalt: A pre-
634 injection overview of the CarbFix project. Int. J. Greenh. Gas Cont. 4, 537-545.

635 Global CCS Institute, 2011. Economic Assessment of Carbon Capture and Storage
636 Technologies: 2011 Update.
637 https://hub.globalccsinstitute.com/sites/default/files/publications/12786/economic-
638 assessment-carbon-capture-and-storage-technologies-2011-update.pdf

639 Goldberg, D.S., Takahashi, T., Slagle, A.L., 2008. Carbon dioxide sequestration in deep-
640 sea basalt. Proc. Nat. Acad. Sci. 105, 9920-9925.

641 Gudbrandsson, S., Wolff-Boenisch, D., Gislason, S.R., Oelkers, E.H., 2011. An
642 experimental study of crystalline basalt dissolution from 2<pH<11 and temperatures
643 from 5 to 75 ^{o}C. Geochim. Cosmochim. Acta 75, 5496-5509.

644 Gunnarsson G., Arnaldsson, A.,.Oddsdóttir, A.L, 2011. Model Simulations of the Hengill
645 Area, Southwestern Iceland. Transport in Porous Media 90, 3–22.

646 Gunnarsson, I., Arnórsson, S., 2000. Amorphous silica solubility and the thermodynamic
647 properties of H_4SiO_4 in the range of 0 to 350 °C at P-sat. Geochim. Cosmochim. Acta
648 64, 2295–2307.

649 Gunnlaugsson, E., 2012. The Hellisheidi geothermal project – Financial aspects of
650 geothermal development. Presented at *Short Course on Geothermal Development and*
651 *Geothermal Wells, UNU-GTP and LaGeo*. http://www.os.is/gogn/unu-gtp-sc/UNU-
652 GTP-SC-14-12.pdf

653 Gysi, A.P., 2017. Numerical simulations of CO_2 sequestration in basaltic rock formations:
654 Challenges for optimizing mineral-fluid reactions. Pure App. Chem. 89, 581-596.

655 Gysi, A.P., Stefansson. A. 2012. CO_2-water-basalt interaction. Low temperature
656 experiment and implications for CO_2 sequestration into basalts. Geochim. Cosmochim.
657 Acta 81, 129-152.

658 Hebach, A., Oberhof, A., Dahmen, N., 2004. Density of water plus carbon dioxide at
659 elevated pressures: Measurements and correlation. J. Chem. Eng. Data 49, 950-953.

660 Hu, B and Zhai, H. 2017. The cost of carbon capture and storage for coal-fired power plants
661 in China. Int. J. Greenh. Gas Control 65, 23–31.

662 IEA, 2015. Energy Technology Perspectives - Mobilizing Innovation To Accelerate
663 Climate Action International Energy Agency, Paris, France.

664 http://www.iea.org/publications/freepublications/publication/energy-technology-
665 perspectives-2015.html

666 IEA, 2016. Electricity information, 2016 edition. International Energy Agency.
667 http://wds.iea.org/wds/pdf/Ele_documentation.pdf

668 Jové Colón C. F., Oelkers, E.H., Schott, J.S., 2004. Experimental investigation of the effect
669 of dissolution on sandstone permeability, porosity, and reactive surface area. Geochim.
670 Cosmochim. Acta 68, 805-817.

671 Kanakiya, S., Adam, L., Esteban, L., Rowe, M.C., Shane, P., 2017. Dissolution and
672 secondary mineral precipitation in basalts due to reactions with carbonic acid. J.
673 Geophys. Res. Solid Earth 122, 4312-4327.

674 Keleman, P.B., Matter, J. 2008. In situ carbonation of peridote for CO_2 storage. PNAS 105,
675 17295-17300.

676 Kervevan, C., Beddelem, M.-H., O'Neil, K., 2014. CO2-DISSOLVED: A novel concept
677 coupling geologic storage of dissolved CO_2 and geothermal heat recovery – Part 1.
678 Assessment of the integration of an innovative low-cost, water based CO_2 Capture
679 technology. Energy Procedia 63, 4508-4518.

680 Kervevan, C., Beddelem, M.-H., Galigue, X., Le Gallo, Y., May, F., O'Neil, K.,
681 Sterpenich, J., 2017. Main results of the CO2-DISSOLVED Project: First step toward
682 a future industrial pilot combining geologic storage of dissolved CO_2 and geothermal
683 heat recovery. Energy Procedia 114, 4086-4098.

Kristjánsson, B.R., Axelsson, G., Gunnarsson, G., Gunnarsson, I., Óskarsson, F., 2016. Comprehensive tracer testing in Hellisheidi Geothermal field in SW-Iceland. Proc. 41st Workshop on Geothermal Engineering, Stanford University.

Luhmann, A.J., Tutolo, B. M., Tan, C.Y., Moskowitz, B.M., Saar, M.O., Seyfried, W.E., 2017. Whole rock basalt alteration from CO_2-rich brine flow through experiments at 150 °C and 150 bar. Chem. Geol. 453, 92-110.

Matter, J. M. Stute, M. Snæbjörnsdottir, S. Ó., Oelkers, E.H. Gislason, S.R. Aradottir, E.S., Sigfusson, B., Gunnarsson, I., Sigurdardottir, H., Gunnlaugsson, E., Axelsson, G., Alfredsson, H. A., Wolff-Boenisch, D., Mesfin, K. de la R. Taya, D.F., Hall, J., Dideriksen, K., Broecker, W.S., 2016. Rapid carbon mineralization for permanent disposal of anthropogenic carbon dioxide emissions. Science 352, 1312-1314.

Maskell, A., Kampman, N., Chapman, H., Condon, D.J., Bickle, M., 2015. Kinetics of CO_2-fluid-rock reactions in a basalt aquifer, Sosa Springs, Idaho, App. Geochem. 61, 272-283.

McGrail, P.B., Schaef, H.T., Ho, A.M., Chien, Y.,-J., Dooley, J. J., Davidson, C. L., 2006. Potential for carbon dioxide sequestration in flood basalts. J. Geoph. Res.; Solid Earth 111, B12201, doi:10.1029/2005JB004169.

Neveu, M., Desch, S.J., Castillo-Rogez, J. C., 2017. Aqueous geochemistry in icy world interiors: Equilibrium fluid, rock, and gas compositions, and fate of antifreezes and radionuclides Geochim. Cosmochim. Acta 212 324–371,

Nogues, J.P., Fitts, J.P., Celia, M.A., Peters, C.A. 2013. Permeability evolution due to dissolution and precipitation of carbonates using reactive trtsansport modeling in pore networks. Water Resources Res. 49, 6006-6021.

Noiriel, C., Steefel, C.I., Yang, L., Bernard, D., 2016. Effects of pore-scale precipitation on permeability and flow. Advances Water Resources 95, 125-137.

Oelkers, E.H. 1996. Physical and chemical properties of rocks and fluids for chemical mass transport calculations. Rev. Min. Geochem. 34, 313-191.

Oelkers E.H., Gislason, S.R., Matter, J.M., 2008. Mineral carbonation of CO_2. Elements 4, 333-337.

Olkawa, K., Yongsiri, C., Takeda, K., Harimoto, T., 2003. Seawater flue gas desulfurization: Its technical implication and performance result. Environ. Prog. 21, 67-71.

Parkhurst, D. L. and Appelo, C. A. J. (2013) *Description of input and examples for PHREEQC. Version 3–a computer program for speciation, batch-reaction, one-dimensional transport, and inverse geochemical calculations.* U.S. Geological Survey Techniques. Methods Report, book 6, chapter A43, pp. 1-497.

Patel, M.R., Eubank, P.T., 1988. Experimental densities and thermodynamic properties of carbon dioxide water mixtures. J. Chem. Eng. Data 33, 185-192.

Pool, M., Carrera, J., Vilarrasa, V., Silva, O., Ayora, C., 2013. Dynamics and design of systems for geological storage of dissolved CO_2. Advances in Water Resources 62, 533-542.

Pham, V., Hai. T., Aagaard, P., Hellevang, H., 2012. On the potential for CO_2 mineral storage in continental flood basalts – PHREEQC batch and 1D diffusion-reaction simulations. Geochem. Trans. 13, 5. DOI: 10.1186/1467-4866-13-5.

Reykjavík Energy, 2016. Environmental report 2016. https://www.or.is/sites/or.is/files/or_environmental_report_2016.pdf

Rose, P.E., Johnson, S., Kilbourn, P., Kastler, C., 2002. Tracer testing at Dixie Valley, Nevada using 1-naphtalene sulfonate and 2,6-napthalene disulfonate. *Proc.26th Workshop on Geothermal Engineering, Stanford University*. https://www.geothermal-energy.org/pdf/IGAstandard/SGW/2002/Rose.pdf?

Rosenbauer, R.J., Thomas, B., Bischoff, J.L., Palandri, J., 2012. Carbon sequestration via reaction with basaltic rocks: Geochemical modeling and experimental results. Geochim. Cosmochim. Acta 89, 116-133.

Rubin, E.S., Davidson, J.E., Herzog, H.J., 2015. The cost of CO_2 capture and storage. Int. J. Greenhouse Gas Cont. 40, 378-400.

Schaef, H.T., Horner, J.A., Owen, A.T., Thompson. C.J., Lorring, J.S., McGrail, B.P., 2014. Mineralization of basalts in the CO_2-H_2O-SO_2-O_2 system. Environ. Sci. and Technol. 48, 5298-5305.

Schaef, H.T., McGrail, B.P., Owen, A.T., Arey, B.W., 2013. Mineralization of basalts in the CO_2-H_2O-H_2S system. Int. J. Greenh. Gas Control 16, 187-196.

Sigfusson, B., Gislason, S.R., Matter, J. M., Stute, M., Gunnlaugsson, E., Gunnarsson, I., Aradottir, E.S., Sigurdardottir, H., Mesfin, K. G., Alfredsson, H. A., Wolff-Boenisch, D., Arnarson, M.T., Oelkers, E.H., 2015. Solving the carbon-dioxide buoyancy challenge: the design and field testing of a dissolved CO_2 injection system. Int. J. Greenh. Gas Control 37, 213–219.

Skippen, G.B. 1980. Dehydration and decarbonation equilibria. In Greenwood H.J. ed. Application of thermodynamics to petrology and ore deposits. Min. Soc. Canada Short Corse. Toronto Canada, Evergreen Press, p. 66-83.

Snæbjörnsdóttir S.Ó., 2011. The Geology and Hydrothermal Alteration at the Western Margin of the Hengill Volcanic System" MSc thesis (in Icelandic), University of Iceland.

Snæbjörnsdóttir, S. Ó., Oelkers, E. H., Mesfin, K., Aradóttir, E.S., Dideriksen, K., Gunnarsson, I., Gunnlaugsson, E., Matter, J.M., Stute, M., Gislason, S.R. 2017. The chemistry and saturation states of subsurface fluids during the in situ mineralization of CO_2 and H_2S at the CarbFix site in SW-Iceland. Int. J. of Greenh. Gas Cont. 58. 87–102.

Snæbjörnsdóttir, S. Ó., Gislason, S. R., Galeczka, I. M., Oelkers, E. H., 2018. Reaction path modelling of in-situ mineralisation of CO_2 at the CarbFix site at Hellisheidi, SW-Iceland. Geochim. Cosmochim. Acta 220, 348-366.

Snæbjörnsdóttir, S. Ó., Wiese, F., Fridriksson, T., Ármannsson, H., Einarsson, G.M., Gislason, S. R., 2014. CO_2 storage potential of basaltic rocks in Iceland and the oceanic ridges. Energy Procedia 63, 4585-4600.

766 Stefánsson, A., Arnórsson, S., Gunnarsson, I., Kaasalainen, H., Gunnlaugsson, E., 2011.
767 The geochemistry and sequestration of H_2S into geothermal system at Hellisheidi,
768 Iceland. J. Volcanol. Geotherm. Res. 202, 179-188.

769 Takazo, S., Yoshizaki, M., Masaki, Y., Suzuki, K., Takai, K., Russell, M.J., 2013.
770 Reactions between basalt and CO_2-rich seawater at 250 and 350 ^{o}C, 500 bars:
771 Implications for the CO_2 sequestration into the modern oceanic crust and the
772 composition of hydrothermal vent fluid in the CO_2-rich early ocean. Chem. Geol. 359,
773 1-9.

774 Tao, Q., and Bryant, S.L., 2014. Optimization of injection/extraction rates for surface-
775 dissolution. SPE Journal 19, 598-607.

776 Teng, H., Yamasaki, A., Chun, M. K., Lee, H., 2007. Solubility of liquid CO_2 in water at
777 temperatures from 278 to 293 and pressures from 6.44 MPa to 29 MPa and densities of
778 corresponding aqueous solutions. J. Chem. Thermo. 29, 1301-1310.

779 Trias, R., Menez, B., Campion, P. Zivanovic,Y., Lecourt, L.,Lecoeuvre, A., Schmitt-
780 Kopplin, P., Uhl, J., Gislason. S.R., Alfredsson, H.A., Mesfin, K.G., Snæbjörnsdóttir,
781 S. Ó., Aradottir, E.S., Gunnarsson, I., Matter, J.M., Stute, M., Oelkers E.H., Gerard, E.
782 2017. High reactivity of deep biota under anthroprogenic CO2 injection into basalt.
783 Nature Comm. 8, 1063.

784 UK Oil and Gas Industry Association, 2016. Oil & Gas UK: Environmental report. The
785 UK Oil and Gas Industry Association Limited 58 pp. http://oilandgasuk.co.uk/wp-
786 content/uploads/2016/11/Environment-Report-2016-Oil-Gas-UK.pdf.

787 U.S. Department of Energy, 2013. More Economical Sulfur Removal for Fuel Processing
788 Plants. Energy Efficiency & Renewable Energy.
789 http://energy.gov/sites/prod/files/2013/11/f5/tda_sbir_case_study_2010.pdf

790 Weiss, RF. 1974. Carbon dioxide in water and seawater: the solubility of a non-ideal gas.
791 Marine Chem. 2, 203-215.

792 Wolff-Boenisch, D., Gislason, S.R., Oelkers, E.H., Putnis, C.V., 2004. The dissolution of
793 natural glasses at pH 4 and 10.6. and temperatures from 25 to 74 ^{o}C. Geochim.
794 Cosmochim. Acta 68, 4843-4858.

795 Wolff-Boenisch, D., Gislason, S.R., Oelkers, E.H., 2006. The effect of crystallinity on
796 dissolution rates and CO_2 consumption capacity of silicates. Geochim. Cosmochim.
797 Acta 70, 858–870.

798 Wolff-Boenisch, D., Wenau, S., Gislason, S.R., Oelkers, E.H., 2011. Dissolution of basalts
799 and peridotite in seawater, in the presence of ligands, and CO_2: Implications for mineral
800 sequestration of carbon dioxide. Geochim. Cosmochim. Acta 75, 5510−5525.

801 Xiong, W., Wells, R. K., Menefee, A. H., Skemer, P., Ellis, B. R., Giammar, D. E., 2017.
802 CO_2 mineral trapping in fractured basalt. Int. J. of Greenh. Gas Cont. 66, 204-217.